

## Numerical simulation of liquefaction susceptibility of soil interacting by single pile

Ahmad Asaadi\* and Mohammad Sharifipour

*Department of Civil Engineering, Faculty of Engineering, Razi University, Kermanshah, Iran.*

Received 08 Jan 2015; received in revised form 16 Apr 2015; accepted 21 Apr 2015

\*Corresponding Author Email: [a.asaadi@pgs.razi.ac.ir](mailto:a.asaadi@pgs.razi.ac.ir), Tel: +989186598192

### Abstract

Previous case histories have shown that soil liquefaction severely damaged many structures supported on pile foundations during earthquakes. As a result, evaluating the potential for instability is an important consideration for the safe and resistant design of deep foundation against earthquakes. In this study, the liquefaction susceptibility of saturated sand interacting by single concrete pile was simulated by means of finite difference method. A nonlinear effective stress analysis was used to evaluate soil liquefaction, and the soil-pile interaction was considered using interface elements. The parameter  $R_u$  was defined as the pore water pressure ratio to investigate liquefaction in the soil mass during time. A set of numerical models were carried out by three types of soil mass with various condensation (loose, semi-dense and dense) under three ground motion with different predominant frequencies and peak accelerations. The effect of these parameters was studied using excess pore pressure, lateral movement and settlement time histories. It was found that the pile can affect the liquefaction susceptibility of soil by comparing the near pile and free field responses. However, for various soil and earthquake characteristics, it was found that the depth of soil liquefaction and triggering, varies.

**Keywords:** *dynamic behavior of pile, excess pore pressure ratio, liquefaction susceptibility, soil-pile interaction.*

### 1. Introduction

The prediction of liquefaction and the resulting displacements is a major concern for earth structures, located in regions of moderate to high seismicity [1]. This is particularly so for superstructures where large displacements and other types of geotechnical instability

could raise life safety concerns. Previous studies have shown that liquefaction induced large lateral displacement severely damaged many structures supported on pile foundations during earthquakes. Therefore, evaluating the potential for instability caused by the

development of excess pore pressure is an important consideration for the safe and resistant design of deep foundation against earthquakes. Liquefaction was reported as the main cause of damage to pile foundations during major earthquakes, such as the 1964 Niigata, 1989 Loma-Prieta, 1995 Kobe, and recent 2011 Tohoku [2-4]. Field experience during the past earthquakes [5], indicates that liquefaction mainly occur at depths less than 15 m, and some dynamic centrifuge model testing [6] suggests a depth or confining-stress limitation on the occurrence of liquefaction.

The prediction of seismic response of pile foundations in liquefying soil layers is difficult and there are many uncertainties in the mechanisms involved in soil structure interaction [7]. A wide range of research works have been implemented in the case of liquefaction potential of soil interaction by pile foundations, including the experimental works of Wilson (1998), Yao *et al.* (2004), Haeri *et al.* (2012), and Tokimatsu *et al.* (2005) [8-11], and also various numerical modeling such as Finn and Fujita (2002), Rahmani and Pak (2012), Cheng and Jeremic (2009), Phanikanth *et al.* (2012) and Choobbasti *et al.* (2012) [3, 7, 12-14]. Despite the wide range of studies as regards the efficiency and power of numerical simulation tools, the interest to investigate further, the numerical simulation of liquefaction susceptibility of soil interaction by single pile is on the increase.

The aim of this study was to evaluate the liquefaction susceptibility of saturated sandy soil reinforced by pile foundation during soil liquefaction. For this purpose, a set of numerical models were carried out using a

two-dimensional plain strain finite difference program, *FLAC<sup>2D</sup>* [15]. However, three different soil density and three earthquake time histories data with different predominant frequencies and different peak accelerations were considered for the analysis. The effects of these factors on the liquefaction susceptibility of the soil (include free-field and near pile areas) were evaluated.

## 2. Numerical Simulation

### 2.1. Model geometry and soil properties

A series of numerical analysis were carried out to investigate various factors affecting the liquefaction potential of saturated sandy soil and seismic performance of pile foundation, including soil relative density and the characteristics of excitation frequency and intensity. Using a comprehensive constitutive model is one of the most important parts of numerical simulation of the dynamic behavior of liquefiable soils [7]. In this study, the soil was modeled using nonlinear elastoplastic Mohr-Coulomb constitutive model, and the concrete pile was modeled using linearly elastic pile elements. Tables 1 and 2 present the parameters used in the model for soil and concrete pile, respectively. The finite difference mesh used for simulation is shown in Figure 1. It consists of 600 zones in 12 rows and 50 columns with dimensions equal to 60 m lateral and 15 m in depth. The zones were set finer around the pile for more precision in this area. The pile is discretized into 12 elements with three degrees of freedom (two displacements and one rotation) at each node and is fixed at the bottom in both translational and rotational directions simulating fixed-end type piles.

**Table 1. Material properties of Nevada sand [16]**

Material parameters	Loose sand	Semi-Dense sand	Dense sand
$D_r$ (%)	35	55	75
Density, $\rho_{sat}$ (kg/m <sup>3</sup> )	1948	1988	2030
Porosity	0.432	0.406	0.382
Friction angle, $\phi$ (deg)	30	34	38
Permeability (m/s)	7.07 E-5	6.05 E-5	4.36 E-5
Low strain Shear Modulus, $G$ (Mpa)	23	29	36
Low strain Bulk Modulus, $K$ (Mpa)	49	64	79
$(N_1)_{60}$	7	13	25
Normal ( $k_n$ ) & Shear ( $k_s$ ) Stiffness, (N/m/m)	7.3 E8	9.4 E8	11.5 E8

**Table 2. Concrete pile properties**

<b>Material parameters</b>	
Diameter (m)	0.6
Pile length (m)	15
Density (kg/m <sup>3</sup> )	2500
Modulus of Elasticity, $E_p$ (MPa)	3.0 E4
Moment of inertia, $I_p$ (m <sup>4</sup> )	0.006
Perimeter (m)	1.884
Cross sectional area, $A_p$ (m <sup>2</sup> )	0.283

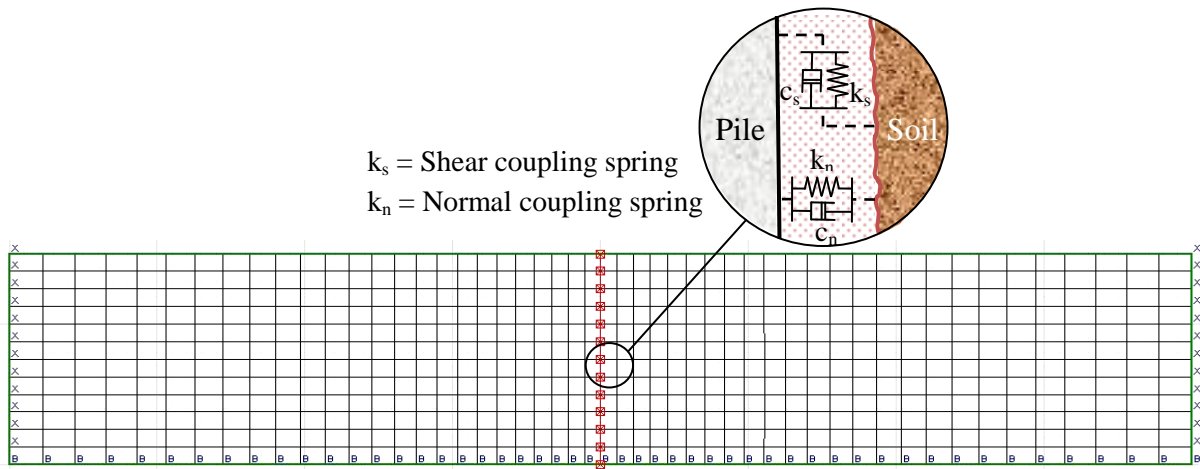


**Fig. 1. Schematic illustration of FDM model of soil interacting pile in FLAC<sup>2D</sup>**

Soil-pile interaction effects were also considered in employing interface elements available in *FLAC<sup>2D</sup>* software. In the present study, the interfaces were modeled via shear  $k_s$  and normal  $k_n$  coupling springs, which were selected at approximately ten times the equivalent stiffness of the stiffest neighboring zone [15]:

$$k_n \text{ or } k_s = 10 \times \max \left[ \frac{K + \frac{4}{3}G}{\Delta Z_{\min}} \right] \quad (1)$$

where,  $K$  and  $G$  are the bulk and shear modulus of the soil zone, respectively, and  $\Delta Z_{\min}$  is the smallest dimension of an adjoining zone in the normal direction. Since the soil is cohesionless, there is no cohesive strength considered in the interface elements, but the frictional resistance of the shear and normal coupling springs were set depending on the friction values of the surrounding soil, which reflect the roughness of the pile surface [15] (about 50-70 percent of the soil friction angle).

Table 1 also summarizes the stiffness properties of the soil-pile interface used in the simulations after adjustment from values calculated by using Equation 1.

### 2.2. Dynamic input

Three different earthquake time history recorded with different predominant frequencies were applied to the base of the model. Each earthquake acceleration time history is scaled as 0.2 and 0.4 g, peak acceleration values. Linear baseline correction was accomplished as the earthquake data histories reached zero displacement at the end of time. Another important thing in dynamic analysis is the wave propagation in the model. Generally, in performing dynamic analyses, the presence of error in the form of wave propagation is likely to happen [17]. The maximum frequency of the shear wave that the model can transmit logically is determined by the Kuhlemeyer and Lysmer (1973) Equation (2) [18]:

$$f = \frac{c_s}{10\Delta l} \quad (2)$$

where  $C_s$  is the shear wave velocity of the soil and  $\Delta l$  is the largest grid zone size in the model. A maximum zone size of 2 m is generated in the model. According to the lowest shear wave velocity related to the soil with lowest relative density (loose sand), the highest admissible frequency is 5 Hz. Hence,

the input earthquake records were filtered by a low pass filter to remove the frequency components higher than 5 Hz. These two corrections were assigned to the time histories of earthquake acceleration, using the well-known SeismoSignal software [19]. The characteristics and fast Fourier transform of earthquake records are presented in Table 3 and Figure 2, respectively.

**Table 3. Earthquake data used in the analysis**

Earthquake Record	Kocaeli (Turkey)	Kobe (Japan)	Bam (Iran)
Recording station	Yarimca	Kakogaw,	Bam
Date of occurrence	(KOERI330)Aug,17,1999	(CUE90)Jan,16,1995	Dec,26,2003
Predominant Frequency (Hz)	0.29	0.95	4.1
Significant duration , ( $D_{5-95}$ ) (sec)	14.6	11.84	9.04
Moment magnitude of earthquake (Mw)	7.4	6.9	6.5

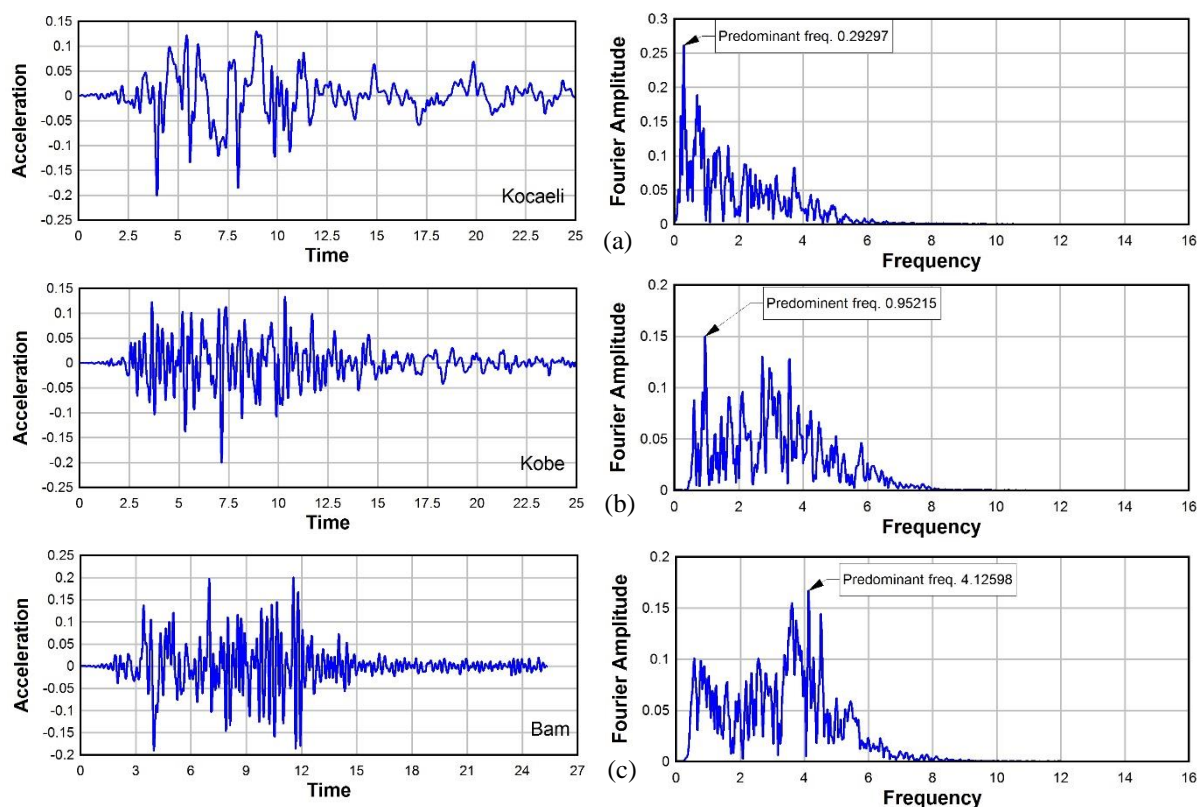


**Fig.2. Acceleration history and their fast Fourier transforms for: (a) Kocaeli, (b) Kobe, and (c) Bam earthquake**

### 2.3. Analysis approach

Generally, the model analysis was performed in three phases. First, the soil elements were loaded under a geostatic condition to obtain the natural steady state. These values were

used as initial stress for the next calculations. Then, the single concrete pile was placed in the soil and the interface properties were applied and thus, the model was analyzed again. In the static analysis, the soil- pile

system was under gravity loading only, the base boundary was fixed in all directions and the side boundaries were fixed in the x direction. Finally, the seismic analysis was carried out. To reduce the reflected waves from the model boundaries, the free-field boundary was used.

Rayleigh damping was used in the numerical analyses herein. The two terms of Rayleigh damping (mass and stiffness) depend on frequency, but it is considered to be frequency independent over a range of predominant frequencies of a response, referred to as a typical velocity record. The idea is to obtain the right damping by adjusting the center frequency ( $f_c$ ) of Rayleigh damping, so that its range coincides with the important frequency. For a problems, such as the dynamic analysis of underground structures, the important frequencies are related to the natural mode of system oscillation [15]. With this background, the important frequency of the present study was estimated by undamped elastic simulations.

In the case of choosing the damping ratio ( $\zeta$ ), because the analysis uses the plasticity constitutive model involving a large strain (that is, Mohr-Coulomb), a considerable amount of energy dissipation can occur during plastic flow. Thus, only a minimal percentage of damping (e.g., 0.5%) may be required [15]. Note that the pile also conform with the stiffness damping that is included by *FLAC*'s default for pile coupling springs.

## 2.4. Liquefaction modeling

Liquefaction is caused by the tendency of granular soil to condense when subjected to monotonic or cyclic shear loading. When this condensation is prevented or curtailed by the presence of water in the pores, normal stress is transferred from the soil skeleton to the water. This can cause high, excess pore pressures resulting in a very large reduction in shear stiffness. This mechanism is well-described by Byrne (1991) [20] who proposed the following empirical equation:

$$\frac{\Delta \varepsilon_{vd}}{\gamma} = c_1 \exp\left(-c_2 \frac{\varepsilon_{vd}}{\gamma}\right) \quad (3)$$

where  $\Delta \varepsilon_{vd}$  is the increment of volume decrease,  $\gamma$  is the cyclic shear-strain, and  $c_1$

and  $c_2$  are constants dependent on the volumetric strain behavior of sand. These constants can be derived from the relative density,  $D_r$ , as:

$$c_1 = 7600 (D_r)^{-2.5} \quad (4)$$

$$c_2 = \frac{0.4}{c_1} \quad (5)$$

This definition is available in *FLAC*, as a built-in model (named Finn model) that incorporates Equation 3 into the standard Mohr-Coulomb plasticity model. The Finn model was used in the present study for pore pressure generation modeling, during seismic analysis.

## 3. Results and Discussion

In this study, the effects of soil type (in terms of relative density), earthquake maximum amplitude, and predominant frequency on liquefaction susceptibility of the soil were evaluated at free-field and near pile areas. The pile response and ground settlement were also investigated. The results are thus discussed as follows.

### 3.1. Effects of soil relative density

Three soil type with different relative densities ( $D_r = 35\%$ ,  $55\%$  and  $75\%$ ) were used in the analysis. The excess pore water pressure ratio ( $R_u$ ) was defined for the software by a Fish function as shown in Equation 6, in which the soil was in the state of liquefaction for  $R_u=1$ ;

$$R_u = \frac{\Delta u}{\sigma'_{vo}} \quad (6)$$

where  $\Delta u$  is the difference between the current and hydrostatic pore pressure, and  $\sigma'_{vo}$  is the initial vertical effective stress. Figure 3 shows the maximum  $R_u$  that was experienced in the soil profile, during the Bam earthquake, when the peak ground acceleration (PGA) was 0.2 g. It was observed that the liquefaction susceptibility of the soil decreases in depth with increase in the soil relative density and this is in line with previous studies. It is also well-illustrated that the soil surrounding the pile experienced less excessive pore water pressure, which is a result of less shear deformation due to the reinforcement effect of pile foundation.

Figure 4 shows the variation of maximum  $R_u$  versus depth in free-field and near pile.

In addition to the aforementioned discussion, It can be seen that near the pile, the maximum amount of  $R_u$  is less than 0.95 in all three cases, indicating that soil liquefaction

does not occur theoretically adjacent to the pile. It is noteworthy that the reduction performance of the single pile is almost equal for all three types of soil. It should also be mentioned that similar results were observed for all events.

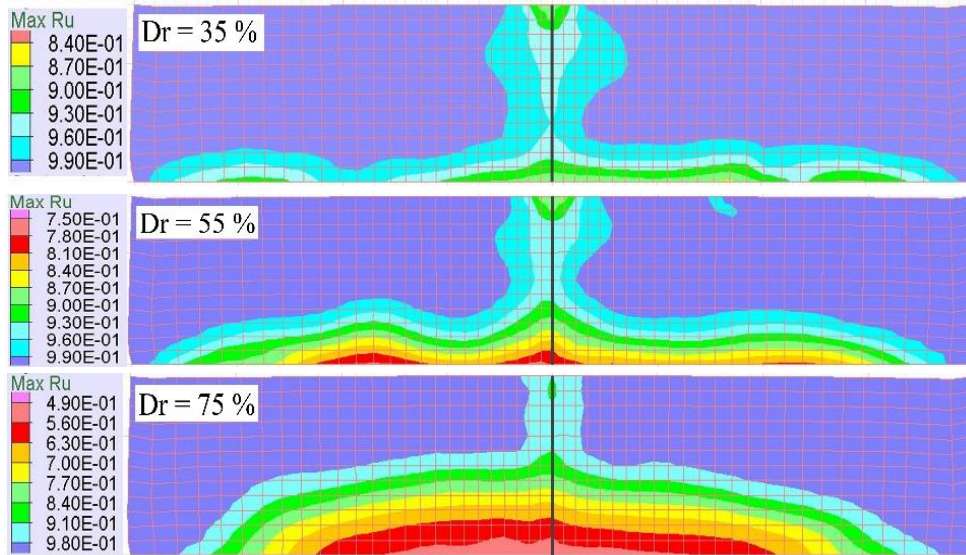


Fig. 3. Maximum  $R_u$  intervals developed in soil profile during Bam earthquake (PGA=0.2g) for various relative density

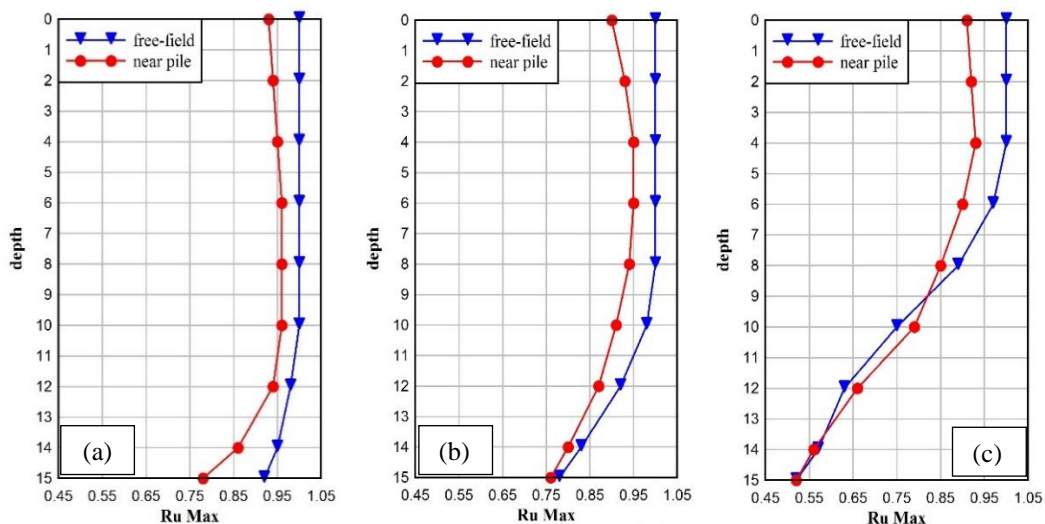


Fig. 4. Variation of maximum  $R_u$  versus depth in free-field and near pile for (a)  $Dr=35\%$ , (b)  $Dr =55\%$ , and (c)  $Dr =75\%$  during Bam earthquake (PGA=0.2g).

### 3.2. Effects of the earthquake maximum amplitude

The Kobe earthquake with two different maximum amplitudes (PGA = 0.2 and 0.4 g) was selected for the input seismic load applied to the model in order to consider the effect of the earthquake peak acceleration. The relative

density of a given soil was considered during the analysis.

Figure 5 (a) and (b) shows the time histories of excess pore pressure ratio at near pile and free-field, respectively with depth of 10 m. The results show that the soil liquefy for both amounts of maximum amplitude, but

liquefaction initiation was faster for PGA=0.4 g. On the other hand, the soil near pile did not liquefy in both cases ( $R_u < 0.95$ ). It is noteworthy that the time history of excess pore pressure ratio near the pile has smoother diagram rather than free-field, and this could be attributed to the stiffer nature of the pile, preventing quick changes in pore water pressure value.

The horizontal displacements at the pile head and the settlement time histories of the soil around the pile are presented in Figure 6 (a) and (b), respectively. As expected, by increasing the maximum amplitude of the earthquake, the deformation increased both horizontally and vertically. It was observed that the maximum horizontal displacement at the pile head were 34 and 44 mm for PGA=0.2 and 0.4 g, respectively (absolute peak values). The settlement of the soil around the pile after shaking were 13 mm (for PGA=0.2 g) and 15 mm (for PGA=0.4 g), that is, sizably less than those values for free-field, 80 and 100 mm, respectively (not shown herein). It can be understood that the pile prevents soil settlement because of its usual frictional behavior.

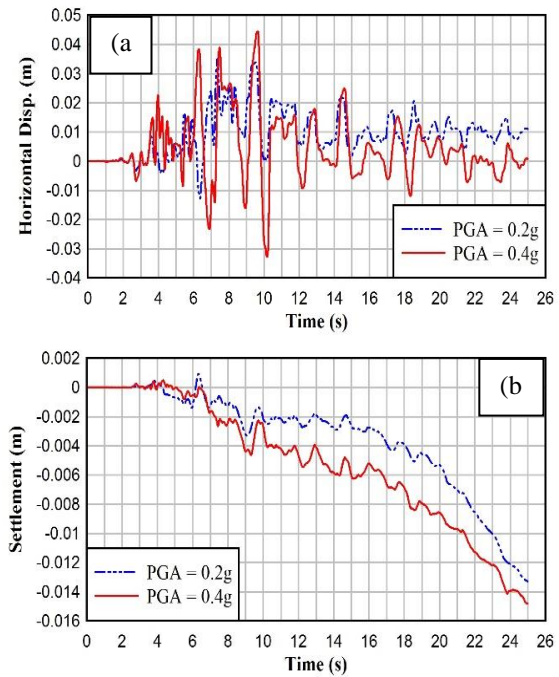


Fig. 6. Computed time histories of: (a) horizontal displacement of pile head, and (b) soil settlement around the pile for different earthquake PGA

Similar results were obtained for each Kocaeli and Bam earthquakes in which the influence of the maximum amplitude was studied.

### 3.3. Effects of the earthquake predominant frequency

Three different earthquake time histories data (Kocaeli, Kobe and Bam) with different predominant frequencies (0.29, 0.95 and 4.1 Hz, respectively) were applied to the model. The analysis was done for a given PGA and soil relative density to consider only the effects of the frequency content.

The results of previous studies discussed earlier were investigated for different earthquake frequencies. It was observed that the liquefaction susceptibility of the soil for both near pile and free-field decreased when the earthquake predominant frequency value increased (Fig. 6 a and b). It is clear that the utmost time at which the main change in pore water pressure begins, is not correlated to the earthquake predominant frequency, in fact it is completely dependent on the first increase in earthquake amplitude (Fig. 2), but the rate of dissipation increased with increase in frequency. It was also observed that the soil near pile did not liquefy as well .

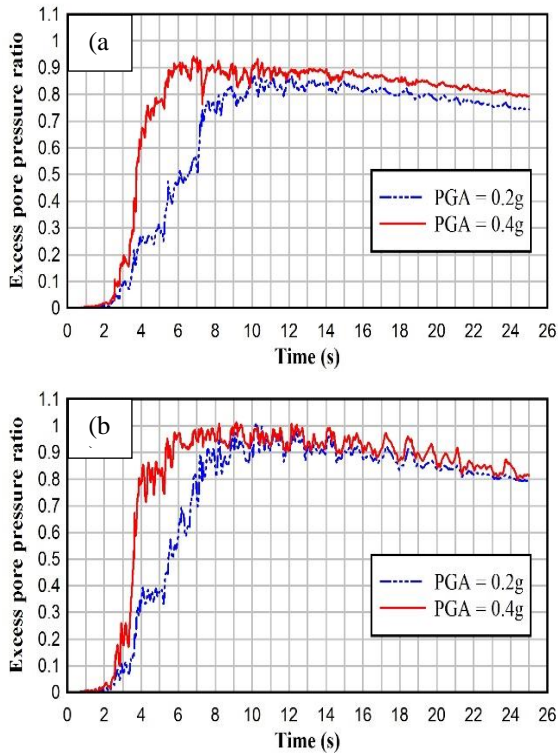
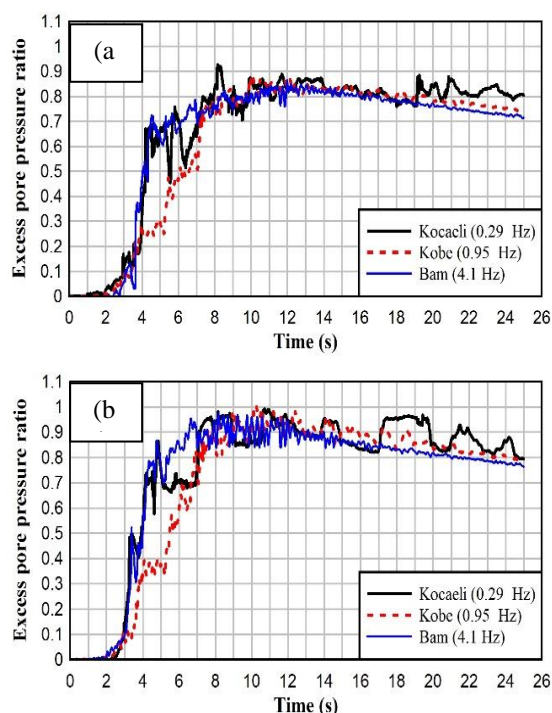


Fig. 5. Computed time histories of: (a) excess pore pressure ratio near the pile, and (b) excess pore pressure ratio at free-field



**Fig.7. Computed time histories of: (a) excess pore pressure ratio near the pile, (b) excess pore pressure ratio at free-field**

The computed results shown in Figure 6 (c) and (d), indicate that the lower frequency causes more deformation both horizontally and vertically. The maximum horizontal displacement of pile head and the maximum settlement of the surrounding soil occurred in the Kocaeli earthquake and are equal to 170 and 24 mm respectively (absolute peak values). However, by comparing the Kobe and Bam earthquake, no significant relationship was observed between the predominant frequency of strong ground motion and the objective deformations in this study, and this could be attributed to other seismic characteristics such as Arias intensity or significant duration.

#### 4. Conclusions

In this study, a series of numerical analysis were carried out to evaluate the effects of soil relative density, earthquake predominant frequency and peak acceleration on the liquefaction susceptibility of soil interaction by single pile and dynamic behavior of the pile in liquefiable soil. Based on the results of this numerical study, the following conclusions can be drawn:

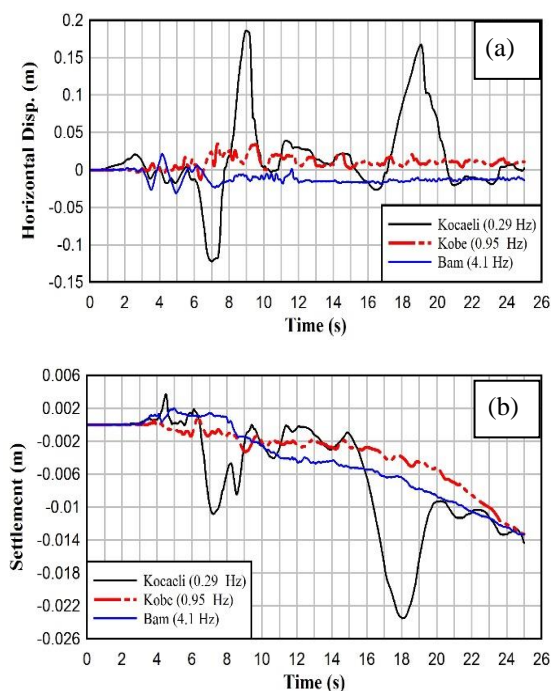


**Fig. 8. Computed time histories of: (a) horizontal displacement of pile head, and (b) soil settlement around the pile for different earthquake with different predominant frequency**

1. Finn constitutive model available in *FLAC<sup>2D</sup>* software was generally capable of calculating the excess pore pressure during earthquake loading, by measurement of irrecoverable volumetric strain. By introducing  $R_u$  as excess pore pressure ratio, the liquefaction phenomenon was specified.

2. For all cases, it was found that liquefaction susceptibility in low depth is more than liquefaction potential in high depth. It was shown that the liquefaction potential of the soil decreases in depth with increase in the soil relative density. In other words, when soil condensation becomes high, the liquefied region moves to the surface therewith.

3. Near the pile, the maximum amount of  $R_u$  was less than 0.95 in all cases indicating that soil liquefaction does not occur theoretically, the pile also generated smoother diagram of pore pressure, thus, it may be interpreted that the pile prevents large shear deformation by soil reinforcement.

4. In considering liquefaction initiation, it was found that liquefaction occurs sooner for higher value of peak ground acceleration. Also, as the maximum amplitude of the earthquake increased, both the pile head

horizontal displacement and surrounding soil settlement increased as well.

5. It was observed that the liquefaction susceptibility of the soil for both near pile and free-field areas decreased when the earthquake predominant frequency value increased and the rate of dissipation increased as the frequency increases.

Generally, this study was unable to find any significant relationship between the earthquake predominant frequency and the objective deformations.

### Acknowledgments

The first author wish to express the extent of his appreciates to the cardiac support of his family, throughout the period of this research.

### References

- [1] Byrne, P. M., Park, S.-S., Beaty, M., Sharp, M., Gonzalez, L., & Abdoun, T. (2004). Numerical modeling of liquefaction and comparison with centrifuge tests. *Canadian Geotechnical Journal*, 41(2), 193-211. doi: 10.1139/t03-088
- [2] Kramer, S. (1996). *Geotechnical earthquake engineering in prentice-Hall international series in civil engineering and engineering mechanics*: Prentice-Hall, New Jersey.
- [3] Finn, W., & Fujita, N. (2002). Piles in liquefiable soils: seismic analysis and design issues. *Soil Dynamics and Earthquake Engineering*, 22(9), 731-742.
- [4] Bhattacharya, S., Sarkar, R., & Huang, Y. (2013). *Seismic Design of Piles in Liquefiable Soils New Frontiers in Engineering Geology and the Environment* (pp. 31-44): Springer.
- [5] Youd, T., Idriss, I., Andrus, R. D., Arango, I., Castro, G., Christian, J. T., . . . Hynes, M. E. (2001). Liquefaction resistance of soils: summary report from the 1996 NCEER and 1998 NCEER/NSF workshops on evaluation of liquefaction resistance of soils. *Journal of Geotechnical and Geoenvironmental Engineering*, 127(10), 817-833.
- [6] Steedman, R. S., Ledbetter, R. H., & Hynes, M. E. (2000). The influence of high confining stress on the cyclic behavior of saturated sand. *Geotechnical Special Publication*, 35-57.
- [7] Rahmani, A., & Pak, A. (2012). Dynamic behavior of pile foundations under cyclic loading in liquefiable soils. *Computers and Geotechnics*, 40(0), 114-126. doi: <http://dx.doi.org/10.1016/j.compgeo.2011.09.002>.
- [8] Yao, S., Kobayashi, K., Yoshida, N., & Matsuo, H. (2004). Interactive behavior of soil-pile-superstructure system in transient state to liquefaction by means of large shake table tests. *Soil Dynamics and Earthquake Engineering*, 24(5), 397-409.
- [9] Tokimatsu, K., Suzuki, H., & Sato, M. (2005). Effects of inertial and kinematic interaction on seismic behavior of pile with embedded foundation. *Soil Dynamics and Earthquake Engineering*, 25(7), 753-762.
- [10] Wilson, D. W. (1998). *Soil-pile-superstructure interaction in liquefying sand and soft clay*. University of California, Davis.
- [11] Haeri, S. M., Kavand, A., Rahmani, I., & Torabi, H. (2012). Response of a group of piles to liquefaction-induced lateral spreading by large scale shake table testing. *Soil Dynamics and Earthquake Engineering*, 38, 25-45.
- [12] Choobbasti, A. J., Saadati, M., & Tavakoli, H. R. (2012). Seismic response of pile foundations in liquefiable soil: parametric study. *Arabian Journal of Geosciences*, 5(6), 1307-1315.
- [13] Phanikanth, V., Choudhury, D., & Reddy, G. (2012). Behavior of single pile in liquefied deposits during earthquakes. *International Journal of Geomechanics*, 13(4), 454-462.
- [14] Cheng, Z., & Jeremić, B. (2009). Numerical modeling and simulation of pile in liquefiable soil. *Soil Dynamics and Earthquake Engineering*, 29(11), 1405-1416.
- [15] Itasca Consulting Group, I. (2011). *FLAC-fast Lagrangian analysis of continua. User's manual, version 7.0*, Minneapolis.
- [16] Popescu, R., & Prevost, J. H. (1993). Centrifuge validation of a numerical model for dynamic soil liquefaction. *Soil Dynamics and Earthquake Engineering*, 12(2), 73-90.
- [17] Asgari, A., Golshani, A., & Bagheri, M. (2014). Numerical evaluation of seismic response of shallow foundation on loose silt and silty sand. *Journal of Earth System Science*, 123(2), 365-379.
- [18] Kuhlemeyer, R. L., & Lysmer, J. (1973). Finite element method accuracy for wave propagation problems. *Journal of Soil Mechanics & Foundations Div*, 99(Tech Rpt).
- [19] Seismosoft. (2013). *SeismoSignal v5.1 – A computer program for signal processing of*

strong-motion data (Version 5.1): available from <http://www.seissoft.com>.

[20] Byrne, P. M. (1991). A cyclic shear-volume coupling and pore pressure model for sand.

Paper presented at the Proc., 2nd International Conference on Recent Advances in Geotechnical Earthquake Engineering and Soil Dynamics, St. Louis.